



Influence of the displacement predictive relationships on the probabilistic seismic analysis of slopes

Fabio Rollo ⁽¹⁾, Sebastiano Rampello ⁽¹⁾

(1) Dipartimento di Ingegneria Strutturale e Geotecnica, Università di Roma *La Sapienza*, via Eudossiana 18, 00184
Roma, Italy

Corresponding Author

Dr. Fabio Rollo

fabio.rollo@uniroma1.it

Tel: +39 06 44585 5957

E-mail addresses:

fabio.rollo@uniroma1.it (F. Rollo; ORCID:0000-0003-2526-8997),

sebastiano.rampello@uniroma1.it (S. Rampello; ORCID: 0000-0003-0489-9589).

25 **Abstract**

26 Seismically-induced landslides can often cause severe human and economic losses. Therefore, it is
27 worth assessing the seismic performance of slopes through a reliable quantification of the permanent
28 displacements induced by seismic loading.

29 This paper presents a new semi-empirical relationship linking the permanent earthquake-induced
30 displacements of slopes to one or two synthetic ground motion parameters developed considering the
31 Italian seismicity and a comparison with existing simplified displacement models is illustrated. Once
32 combined with a fully probabilistic approach, these relationships provide a useful tool for practicing
33 engineers and national agencies for a preliminary estimate of the seismic performance of a slope. In
34 this perspective, the predictive capability of different semi-empirical relationships is analysed with
35 reference to the permanent displacements evaluated for the Italian seismicity assimilating the slope
36 to a rigid body and adopting the Newmark's integration approach. The consequences of the adoption
37 of these relationships on the results of the probabilistic approach are illustrated in terms of
38 displacement hazard curves and hazard maps for different slope scenarios.

39

40 *Keywords:* slopes, earthquake-induced displacements, semi-empirical relationships, probabilistic
41 analysis, displacement hazard curves, displacement hazard maps

42 **1 Introduction**

43 The seismic performance of a slope is often evaluated through the permanent displacements
44 developed at the end of the seismic event (Jibson, 2011; Wasowski *et al.*, 2011). A well-established
45 method to quantify the displacements is that proposed by Newmark (1965), that consists to model the
46 slope with a rigid block sliding on a horizontal plane that experiences permanent displacements only
47 when the critical acceleration function of the slope resistance is lower of that of the input motion.

48 In the last two decades several semi-empirical relationships have been proposed, that link the
49 permanent slope displacements computed through the Newmark's method, using different ground
50 motion databases, to a series of ground motion parameters and the yield seismic coefficient k_y
51 denoting synthetically the seismic slope resistance (e.g. Jibson, 2007; Saygili & Rathje, 2008;
52 Rampello *et al.*, 2010; Biondi *et al.*, 2011; Song *et al.*, 2017; Tropeano *et al.*, 2017; Bray *et al.*, 2018;
53 Du *et al.*, 2018a Bray & Macedo, 2019; Cho & Rathje, 2022). Several efforts have been made to
54 produce more reliable semi-empirical relationships through different combination of ground motion
55 parameters (e.g. Chousianitis *et al.*, 2014; Bray & Macedo, 2019) and, more recently, to account for
56 the influence of slope parameters variability (Du *et al.*, 2018b) through machine learning algorithms
57 (e.g. Xiong *et al.*, 2019; Wang *et al.*, 2020; Liu & Macedo, 2022). For instance, to better describe the
58 properties of the earthquake, the parameters Arias intensity I_A and the mean period T_m have been
59 adopted as they can also embody the duration and the frequency content of the ground motion.
60 Moreover, the performance of the semi-empirical relationships increases when more than one ground
61 motion parameter is used (Bazzurro & Cornell, 2002) as they can account for other relevant features
62 of the ground motion that influence the displacements of the slope. These simplified relationships can
63 be used to predict the seismic-induced displacements of specific slopes and embankments (e.g.
64 Meehan & Vahedifard 2013, Kan *et al.*, 2017) but also become a powerful and attractive tool when
65 combined with a fully probabilistic-based approach capable to account for the aleatory variability of
66 earthquake ground motion and displacement prediction (e.g. Rathje & Saygili, 2008, 2011; Bradley,
67 2012; Lari *et al.*, 2014; Du & Wang, 2016; Rodriguez-Marek & Song, 2016; Song *et al.*, 2018;
68 Macedo & Candia, 2020; Macedo *et al.*, 2020; Yeznabad *et al.*, 2022) and the variability of the slope
69 parameters (e.g. Wang & Rathje, 2018; Li *et al.*, 2020; Wang *et al.*, 2021). Within this theoretical
70 framework, scalar and vector probabilistic approaches can be developed if one or more ground motion
71 parameters are considered. Moreover, the probabilistic analysis can be extended at a regional scale
72 using the ground motion hazard information to produce landslides hazard maps that allows to detect
73 the portions of territory that are more susceptible to earthquake-induced slope instability (e.g. Saygili

74 & Rathje, 2009; Wang & Rathje, 2015; Chousianitis *et al.*, 2016; Sharifi-Mood *et al.*, 2017; Li *et al.*,
75 2022).

76 Recently, Rollo & Rampello (2021) adopted this probabilistic approach for the Italian territory,
77 obtaining hazard curves and hazard maps providing the mean annual rate of exceedance λ_d (as an
78 alternative the return period $T_r=1/\lambda_d$) for different values of permanent displacements and yield
79 seismic coefficient k_y , stemming from the seismic database updated by Gaudio *et al.* (2020). In both
80 works, Newmark's integration of the ground motions was performed for the scheme of infinite slope,
81 using different semi-empirical relationships. Although Gaudio *et al.* (2020) show that the most
82 efficient semi-empirical relationships are obtained for the couple of ground motion parameters (I_A ,
83 T_m), it is more convenient to adopt the couple PGA , PGV . In fact, (i) the adoption of the ratio k_y/PGA
84 is crucial to control the behaviour of the model for displacements close to zero or with very high
85 values and (ii) the probabilistic method adopted here requires ground motion predictions equations
86 (GMPE) that are often developed only in terms of PGA and PGV . Moreover, (iii) the method uses the
87 results of a standard seismic probabilistic hazard analysis (PSHA) that are usually presented in terms
88 of peak ground acceleration hazard curves.

89 In this work a new semi-empirical relationship is presented, developed with reference to the Italian
90 seismicity, along the line tracked by Rollo & Rampello (2021), assimilating the slope to a rigid sliding
91 block. Although the Newmark's method ignores the soil deformability and the cyclic degradation of
92 the shear strength, that would require site-specific studies, it represents an attractive tool for the
93 screening level analysis of slopes at the regional scale. The predictive capability of this new
94 relationship is compared with other existing formulations and proves to be more reliable for the
95 assessment of the seismic performance of slopes in Italy. The comparison presented here aims at
96 providing some guidance in the choice of the semi-empirical relationships, highlighting their
97 advantages and drawbacks in predicting the displacements induced by earthquake loading in a slope,
98 and their application within a probabilistic approach. Furthermore, in this study a wider range of yield
99 seismic coefficients is considered with respect to what presented in Rollo & Rampello (2021), to
100 account for a larger number of slope scenarios. The results of the probabilistic approach are first
101 shown in terms of displacement hazard curves considering both the scalar and the vector approaches,
102 highlighting that the results obtained through the latter are not only more reliable but also are less
103 sensitive to the choice of the specific predictive relationships adopted for the earthquake-induced
104 slope displacements. Finally, displacement hazard maps showing the distribution of the return period
105 for different prescribed values of slope displacements and seismic yield coefficient are presented,

106 aimed at clarifying the role of the adopted displacement semi-empirical relationships on the
107 evaluation of the seismic hazard at a regional scale.

108 **2 Displacement predictive relationships under study**

109 The displacement relationships provide the natural log of permanent horizontal displacement d given
110 the natural log of one or more ground motion parameters (GM). In principle, any combination of
111 ground motion parameters can be adopted. However, as discussed by [Rollo & Rampello \(2021\)](#), the
112 parameters PGA and PGV are more suitable for the development of the probabilistic approach
113 requiring a standard seismic probabilistic hazard analysis (PSHA).

114 With this premise, the simplest semi-empirical relationships are those proposed by [Fotopoulou &](#)
115 [Pitilakis \(2015\)](#), reported here for both the scalar and the vector approaches:

$$\begin{aligned}\ln(d) &= a_0 + a_1 \ln(PGA) \\ \ln(d) &= a_0 + a_1 \ln(PGA) + a_2 \ln(PGV)\end{aligned}\tag{1}$$

116 where d is expressed in cm and a_0 , a_1 and a_2 are the regression coefficients. [Eq. \(1\)](#) represents linear
117 relationships between the natural log of displacements and the natural log of the ground motion
118 parameters PGA and PGV . Displacements d are computed by [Eq. \(1\)](#) for given values of the seismic
119 yield coefficient k_y , so that different sets of regression coefficients are obtained depending on k_y .
120 According to [Cornell & Luco \(2001\)](#), the efficiency of the semi-empirical relationships can be
121 quantified by the standard deviation σ_{\ln} of the natural log of displacement. Despite the simplicity
122 and the limits of application of the linear relationships, they are employed here for comparison with
123 more sophisticated predictive equations. [Saygili & Rathje \(2008\)](#) proposed a modification of [Eq. \(1\)](#)
124 employing the following second-order polynomial expressions:

$$\begin{aligned}\ln(d) &= a_0 + a_1 \ln(PGA) + a_2 [\ln(PGA)]^2 \\ \ln(d) &= a_0 + a_1 \ln(PGA) + a_2 [\ln(PGA)]^2 + a_3 \ln(PGV) + a_4 [\ln(PGV)]^2\end{aligned}\tag{2}$$

125 with the addition of the regression coefficients a_2 and a_4 , still depending on k_y , as above. Then, a
126 functional form that encompasses the ratio k_y/PGA has been also proposed by [Saygili & Rathje](#)
127 [\(2008\)](#):

$$\ln(d) = a_0 + a_1 \frac{k_y}{PGA} + a_2 \left(\frac{k_y}{PGA} \right)^2 + a_3 \left(\frac{k_y}{PGA} \right)^3 + a_4 \left(\frac{k_y}{PGA} \right)^4 + a_5 \ln(PGA) \quad (3)$$

$$\ln(d) = a_0 + a_1 \frac{k_y}{PGA} + a_2 \left(\frac{k_y}{PGA} \right)^2 + a_3 \left(\frac{k_y}{PGA} \right)^3 + a_4 \left(\frac{k_y}{PGA} \right)^4 + a_5 \ln(PGA) + a_6 \ln(PGV)$$

128 However, the 4th order polynomial forms of Eq. (3) do not respect the conditions $d \rightarrow \infty$ for k_y/PGA
 129 $= 0$ and $d = 0$ for $k_y/PGA = 1$ expected for the case of rigid block. This is why the expressions that
 130 satisfy the above conditions, proposed by Ambraseys & Menu (1988) and adopted by Rollo &
 131 Rampello (2021), are also reported:

$$\ln(d) = a_0 + a_1 \ln\left(1 - \frac{k_y}{PGA}\right) + a_2 \ln\left(\frac{k_y}{PGA}\right) \quad (4)$$

$$\ln(d) = a_0 + a_1 \ln\left(1 - \frac{k_y}{PGA}\right) + a_2 \ln\left(\frac{k_y}{PGA}\right) + a_3 \ln(PGV)$$

132 In this study, to improve the predictive capability of Eq. (4) while respecting the conditions at the
 133 extrema, a new semi-empirical relationship is proposed:

$$\ln(d) = a_0 + a_1 \ln\left(1 - \frac{k_y}{PGA}\right) + a_2 \ln\left(\frac{k_y}{PGA}\right) + a_3 \left[\ln\left(\frac{k_y}{PGA}\right) \right]^2 + a_4 \ln(PGA) \quad (5)$$

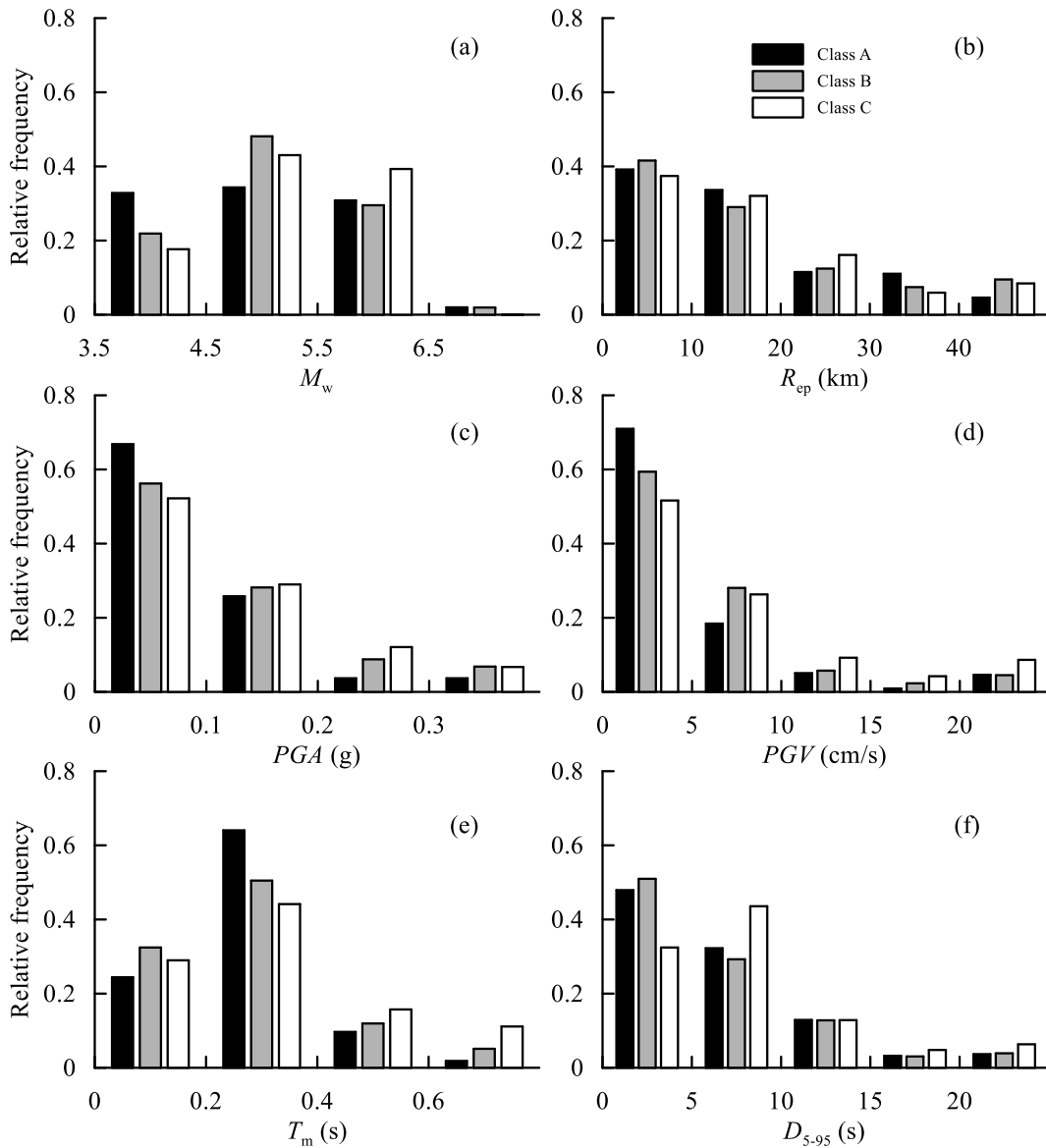
$$\ln(d) = a_0 + a_1 \ln\left(1 - \frac{k_y}{PGA}\right) + a_2 \ln\left(\frac{k_y}{PGA}\right) + a_3 \left[\ln\left(\frac{k_y}{PGA}\right) \right]^2 + a_4 \ln(PGA) + a_5 \ln(PGV)$$

134 These new relationships are simpler than those of Eq. (3) as characterised by one less term (i.e.
 135 one coefficient less to be calibrated) and still allows to predict the permanent displacements for any
 136 value of yield seismic coefficient with a unique set of coefficients.

137 3 Comparison of the displacement relationships for the Italian seismicity

138 In this section the predictive capability of the relationships described above is critically analysed
 139 with reference to the Italian seismicity. A brief description of the seismic database is reported here,
 140 and the readers are referred to Gaudio *et al.* (2020) and Rollo & Rampello (2021) for further details.
 141 The seismic database collects 954 records by 297 stations of the Italian territory and refers to 208

142 earthquakes occurred from 14/06/1972 to 24/04/2017 and characterised by moment magnitude $M_w \geq$
143 4, peak ground accelerations $PGA \geq 0.05$ g and epicentral distance $R_{ep} < 100$ km. Most of the records
144 have peak ground acceleration ranging between 0.05 and 0.2 g while the peak ground velocity from
145 1 and 10 cm/s and the values of the mean period T_m between 0.1 and 0.8 s. Concerning the tectonic
146 aspects, the normal fault with 581 events, equal to 61.3% of the total, is the most common mechanism,
147 followed by the reverse faulting with 170 (18%), the oblique reverse with 126 (13.3%) and strike-slip
148 with 65 (6.9%). According to the Eurocode 8, Part I (CEN 2003), the database is organised in five
149 groups based on the subsoil class of the recording station. In detail, 123 records (13% of the total)
150 refer to rock-like subsoil (class A), 469 (49.5%) to dense and stiff subsoils (class B), 294 (31%) to
151 medium stiff soil (class C), 14 (1.5%) to loose and soft subsoil (class D) and 47 (5%) to weaker
152 materials (class E). Figure 1 shows the distribution of the relative frequency of the quantities M_w , R_{ep} ,
153 PGA , PGV , T_m and D_{5-95} for the subsoil classes A, B and C, while the data from the classes D and E
154 were disregarded as the number of records is only equal to 1.5% and 5% of the total, respectively.

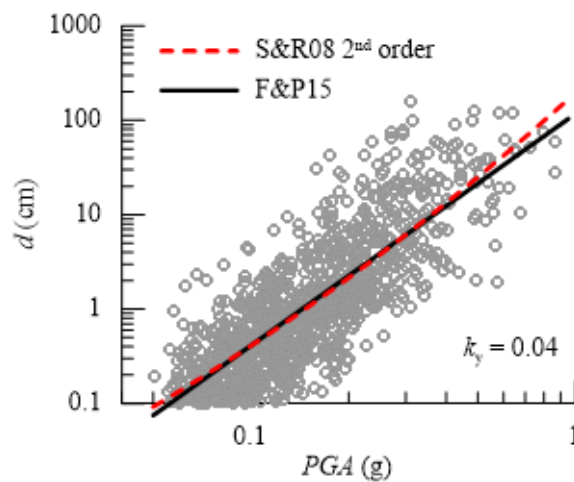


156 Figure 1. Frequency distribution of (a) moment magnitude, (b) epicentral distance, (c) peak ground acceleration, (d) peak ground
 157 velocity, (e) mean period and (f) significant duration for different subsoil classes (after Rollo & Rampello, 2021)

158 **Figure 1** shows that the distributions of the ground motion parameters PGA and PGV are similar,
 159 ranging between 0.05 and 0.1 g and 1 and 5 cm/s, respectively, and, as discusses in the following, are
 160 highly correlated.

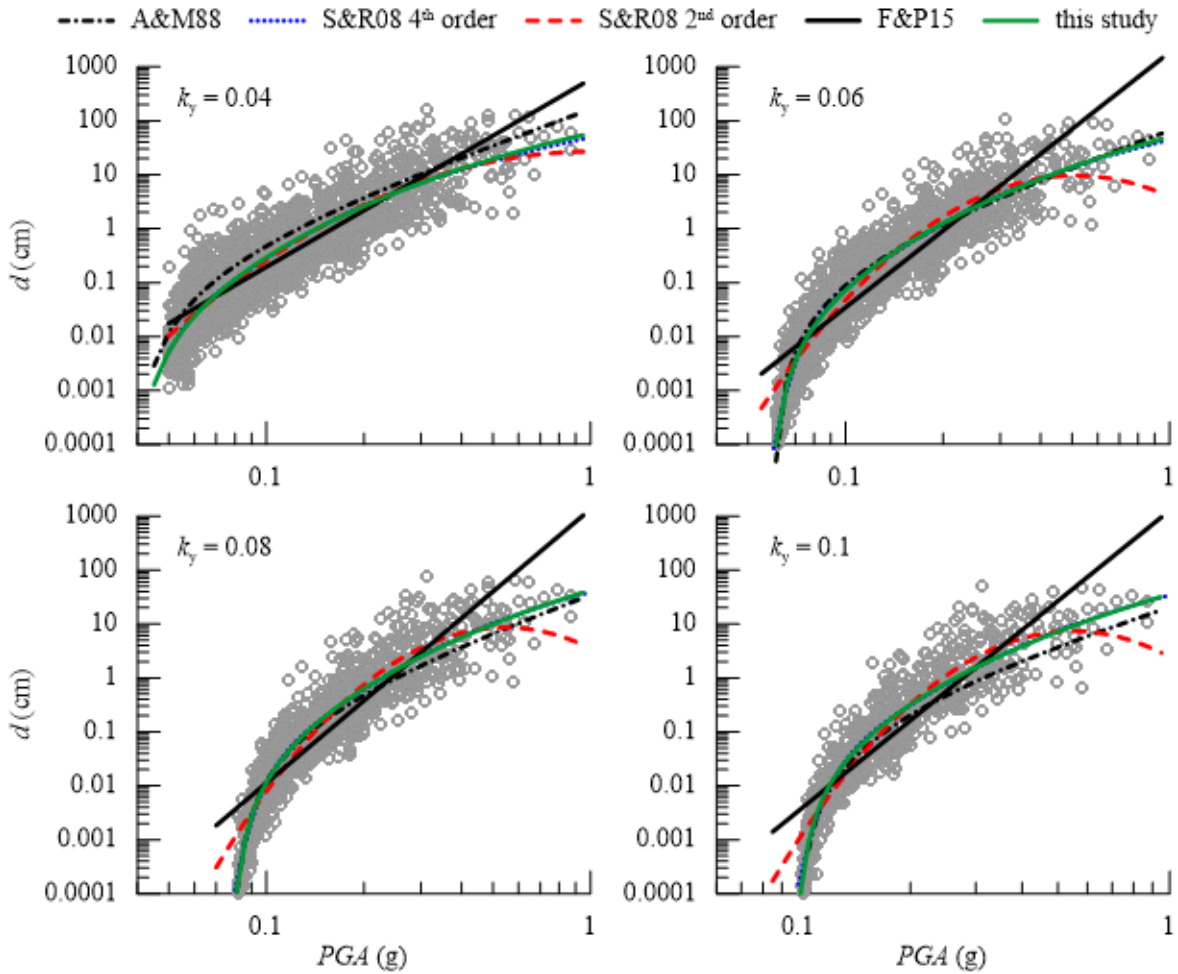
161 According to [Gaudio et al. \(2020\)](#) and [Rollo & Rampello \(2021\)](#), the permanent displacements are
 162 computed with the rigid sliding-block model ([Newmark, 1965](#)) for the simple scheme of an infinite
 163 slope for different values of the yield seismic coefficient, using the updated version of the Italian
 164 strong motion database. Additional values of the seismic coefficient have been considered here with
 165 respect to those investigated by [Rollo & Rampello \(2021\)](#) to increase the representativeness of the
 166 study ($k_y=0.04,0.06,0.08,0.1,0.12,0.15$).

167 The results of the predictive relationships of Eq. (1) proposed by Fotopoulou & Pitilakis (2015)
 168 (F&P15) and Eq. (2) by Saygili & Rathje (2008) (S&R08 2nd order) are first compared for $k_y=0.04$
 169 considering permanent displacements greater than 0.1 cm as lower values are not relevant from an
 170 engineering perspective. The regression coefficients are $a_0 = 4.761$, $a_1 = 2.456$ for the linear case and
 171 $a_0 = 5.277$, $a_1 = 3.093$, $a_2 = 0.179$ for the quadratic law, with the same $\sigma_{ln} = 0.958$. Figure 2 shows
 172 the prediction of the relationships for the single ground motion parameter *PGA* and the dots are the
 173 permanent displacements computed using the Newmark's method.
 174



175 Figure 2. Comparison between the single ground motion parameter (*PGA*) semi-empirical relationships of Eqs. (1) and (2)

176 At a glance, the simplest semi-empirical relationships seem to reproduce satisfactorily the
 177 computed displacements when values greater than 0.1 cm are considered for earthquake-induced
 178 displacements. However, when smaller values of slope displacements are taken into account, the
 179 predictive relationships of Eqs. (1) and (2) fail at reproducing the trend of the computed permanent
 180 displacements. Figure 3 illustrates the results of the scalar relationships for different values of k_y
 181 considering displacements greater than 0.0001 cm. The linear and the quadratic relationships are too
 182 simplistic to capture with sufficient accuracy the variation of d with *PGA*, especially as the yield
 183 seismic coefficient increases. By contrast, the new expression proposed in Eq. (5), as well as the
 184 predictive relationships of Eqs. (3) and (4) proposed by Saygili & Rathje (2008) (S&R08 4th order)
 185 and Ambraseys & Menu (1988) (A&M88), respectively, can nicely reproduce the non-linear variation
 186 of the permanent displacements with *PGA* for any value of k_y , with Eqs. (4) and (5) also predicting
 187 correctly the conditions at the extrema.



189

Figure 3. Comparison of the scalar semi-empirical relationships for different values of k_y

190 [Tables 1-3](#) report the regression coefficients of the semi-empirical relationships evaluated for
 191 computed displacements greater than 0.0001 cm. For the relationships of [Eqs. \(1\)](#) and [\(2\)](#) different
 192 sets of coefficients must be employed for different values of k_y while [Eqs. \(3\) - \(5\)](#) provide a single
 193 set of coefficients valid for any yield seismic coefficient in the range 0.04 to 0.15.

194 [Tables 1-3](#) also collect the standard deviations of the natural log of displacement σ_{\ln} , proving that
 195 for all the adopted expressions, the use of two parameters (PGA , PGV) semi-empirical relationships
 196 reduces substantially the error associated to the computed displacements as compared to the scalar
 197 approach. This result is expected as the couple of ground motion parameters PGA , PGV is more
 198 representative of the Italian seismicity than the PGA alone. Furthermore, the standard deviations
 199 associated to the linear and the quadratic relationships are greater than those computed for the other
 200 relationships, confirming that these latter are more reliable to predict the permanent displacements
 201 for different values of PGA and k_y .

202

203

Table 1. Regression parameters for Eq. (1) for different k_y

F&P15 relationship	GM parameter	a_0	a_1	a_2	σ_{in}
$k_y = 0.04$	<i>PGA</i> (g)	6.378	3.48	-	1.094
	<i>PGA</i> (g), <i>PGV</i> (cm/s)	0.054	1.731	1.596	0.667
$k_y = 0.06$	<i>PGA</i> (g)	7.531	4.731	-	1.288
	<i>PGA</i> (g), <i>PGV</i> (cm/s)	2.163	3.25	1.355	1.059
$k_y = 0.08$	<i>PGA</i> (g)	7.203	5.076	-	1.267
	<i>PGA</i> (g), <i>PGV</i> (cm/s)	1.644	3.501	1.373	1.023
$k_y = 0.10$	<i>PGA</i> (g)	7.143	5.562	-	1.287
	<i>PGA</i> (g), <i>PGV</i> (cm/s)	1.443	3.909	1.386	1.042
$k_y = 0.12$	<i>PGA</i> (g)	6.967	5.938	-	1.333
	<i>PGA</i> (g), <i>PGV</i> (cm/s)	0.697	4.058	1.494	1.047
$k_y = 0.15$	<i>PGA</i> (g)	6.484	6.281	-	1.341
	<i>PGA</i> (g), <i>PGV</i> (cm/s)	0.279	4.453	1.491	1.026

204

205

Table 2. Regression parameters for Eq. (2) for different k_y

S&R08 2 nd order relationship	GM parameter	a_0	a_1	a_2	a_3	a_4	σ_{in}
$k_y = 0.04$	<i>PGA</i> (g)	3.289	0.013	-0.871	-	-	1.038
	<i>PGA</i> (g), <i>PGV</i> (cm/s)	-3.772	-2.505	-1.049	1.476	0.048	0.539
$k_y = 0.06$	<i>PGA</i> (g)	1.371	-2.67	-1.994	-	-	1.083
	<i>PGA</i> (g), <i>PGV</i> (cm/s)	-5.137	-5.385	-2.284	1.097	0.101	0.737
$k_y = 0.08$	<i>PGA</i> (g)	1.262	-2.942	-2.428	-	-	1.063
	<i>PGA</i> (g), <i>PGV</i> (cm/s)	-4.793	-5.362	-2.654	1.073	0.097	0.722
$k_y = 0.10$	<i>PGA</i> (g)	0.893	-675	-3.063	-	-	1.054
	<i>PGA</i> (g), <i>PGV</i> (cm/s)	-4.69	-5.762	-3.194	0.914	0.108	0.725
$k_y = 0.12$	<i>PGA</i> (g)	0.433	-4.631	-3.832	-	-	1.076
	<i>PGA</i> (g), <i>PGV</i> (cm/s)	-4.792	-6.04	-3.693	0.959	0.094	0.740
$k_y = 0.15$	<i>PGA</i> (g)	0.159	-5.273	-4.709	-	-	1.094
	<i>PGA</i> (g), <i>PGV</i> (cm/s)	-4.593	-6.369	-4.449	0.763	0.124	0.737

206

207

Table 3. Regression parameters for Eqs. (3), (4) and (5)

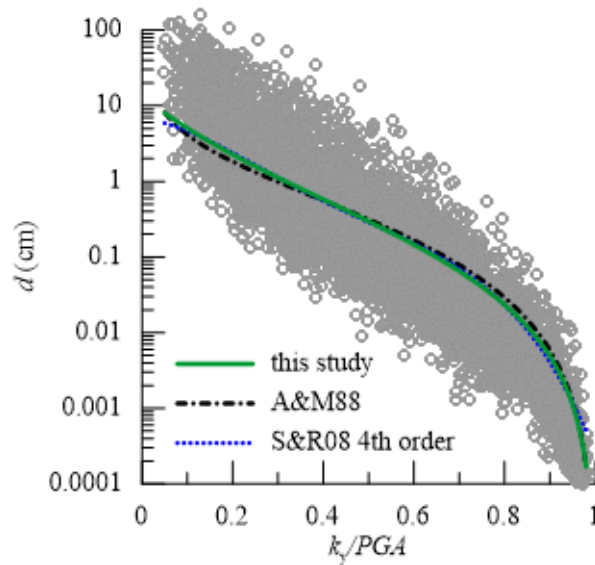
Displacement relationship	GM parameter	a_0	a_1	a_2	a_3	a_4	a_5	a_6	σ_{in}
Ambraseys & Menu (1988)	<i>PGA</i> (g)	-1.667	2.017	-2.127	-	-	-	-	1.103
	<i>PGA</i> (g), <i>PGV</i> (cm/s)	-2.959	2.178	-0.809	1.322	-	-	-	0.579
Saygili & Rathje (2008) 4 th order	<i>PGA</i> (g)	4.104	-4.211	-19.1	41.54	-28.56	1.113	-	1.002
	<i>PGA</i> (g), <i>PGV</i> (cm/s)	-2.241	-1.669	-27.1	52.66	-34.04	-0.556	1.526	0.553
This study	<i>PGA</i> (g)	0.698	1.899	-1.987	-0.285	1.101	-	-	1.001
	<i>PGA</i> (g), <i>PGV</i> (cm/s)	-5.124	1.992	-1.736	-0.234	-0.573	1.531	-	0.547

208

209

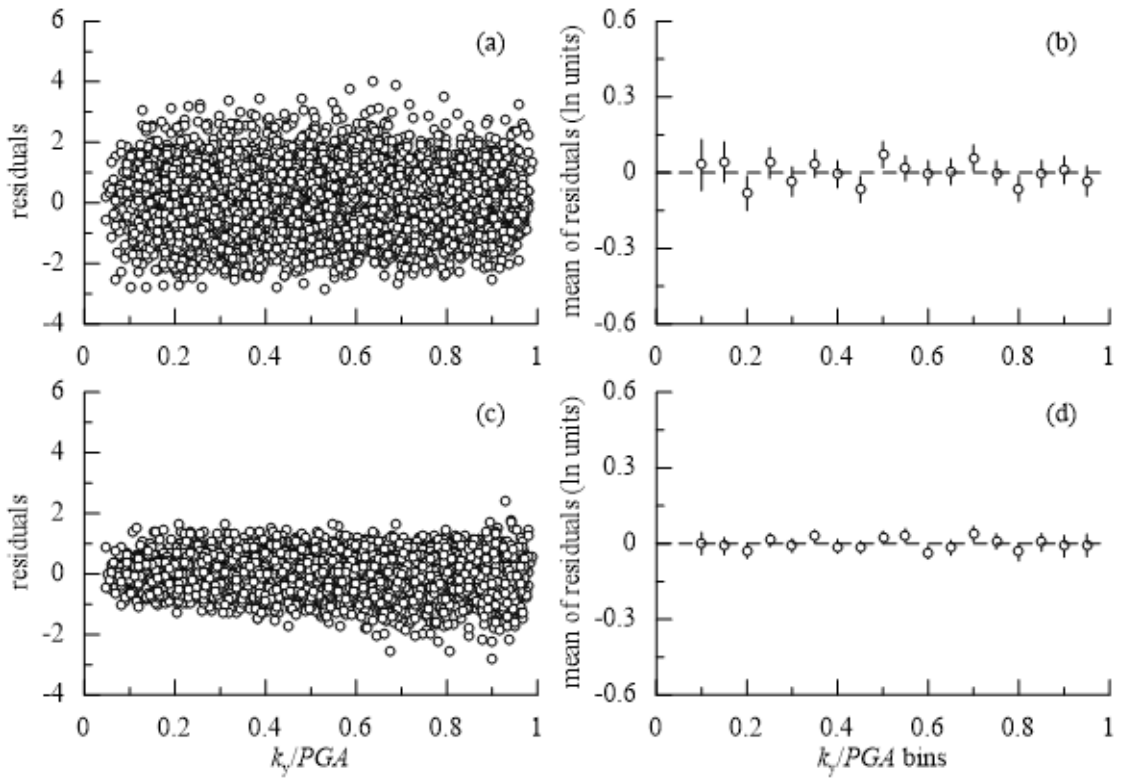
210 In addition, the relationships of Eqs. (3) - (5) are more useful as they provide the permanent
 211 displacements for any value of k_y stemming from a single set of regression coefficients.

212 The results of the vector approach are illustrated in Figure 4 as a function of the ratio k_y/PGA (Eqs.
 213 (3) - (5)). The curves plotted in the figure refer to a value of $PGV = 8$ cm/s, representing the average
 214 value for the seismic database, and demonstrate that the vector approaches provide curves that plot
 215 very close each other.



217 Figure 4. Displacements versus k_y/PGA for vector semi-empirical relationships ($PGV = 8$ cm/s)

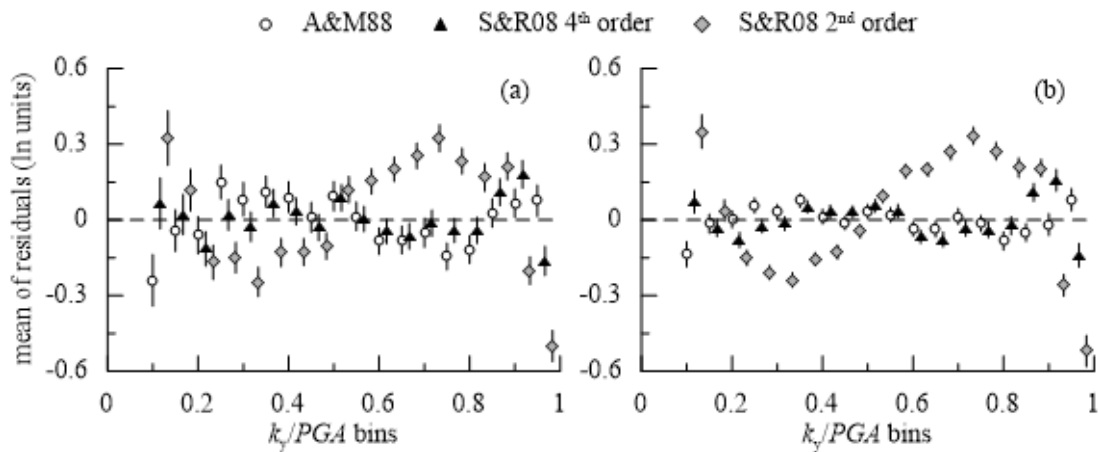
218 Moreover, for both scalar and vector models, it is worth calculating the residuals of the displacements
 219 $\ln d_{\text{observed}} - \ln d_{\text{predicted}}$, with $\ln d_{\text{observed}}$ the displacement evaluated through the Newmark's method
 220 and $\ln d_{\text{predicted}}$ that predicted through the semi-empirical relationships. For the new semi-empirical
 221 relationship, [Figures 5 \(a, c\)](#) show the residuals over the range of k_y/PGA while [Figures 5 \(b, d\)](#) show
 222 the mean of residuals for different k_y/PGA bins, where the vertical bars denote the standard deviation
 223 above and below the mean values. The values of the residuals obtained through the vector approach
 224 are half of those calculated with the scalar one, with irrelevant biases and almost constant standard
 225 deviations over the whole range of k_y/PGA . Again, the vector approach should be preferred as it
 226 predicts lower values of the residuals with respect to the scalar one, with similar trends observed with
 227 increasing k_y/PGA .



229 Figure 5. Mean residuals versus k_y/PGA for scalar approach (a, b) and vector approach (c, d) for the new relationship

230 For comparison, Figure 6 depicts the mean of residuals and their standard deviations obtained through
 231 the expressions of Saygili & Rathje (2008) and Ambraseys & Menu (1988), while the results of the
 232 Eq. (1) are not illustrated as it predicts much greater values of the mean of residuals than the other
 233 equations.

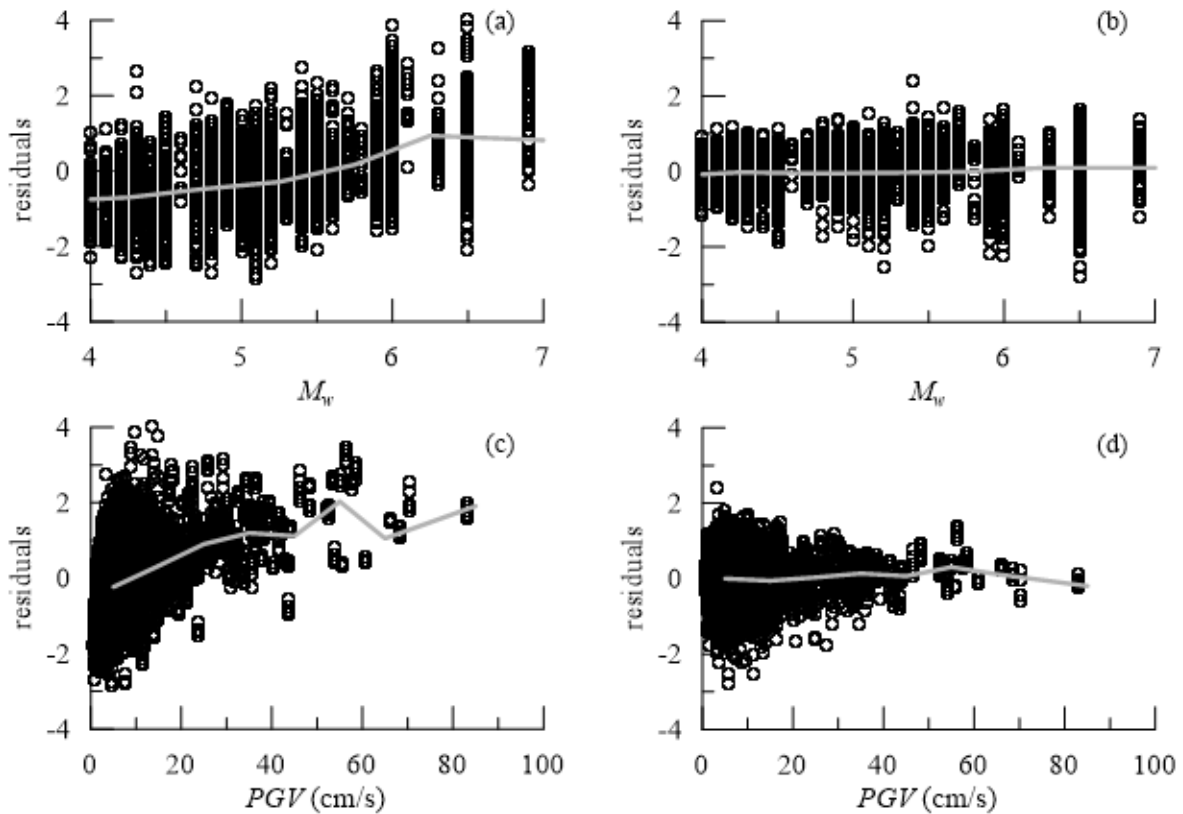
234



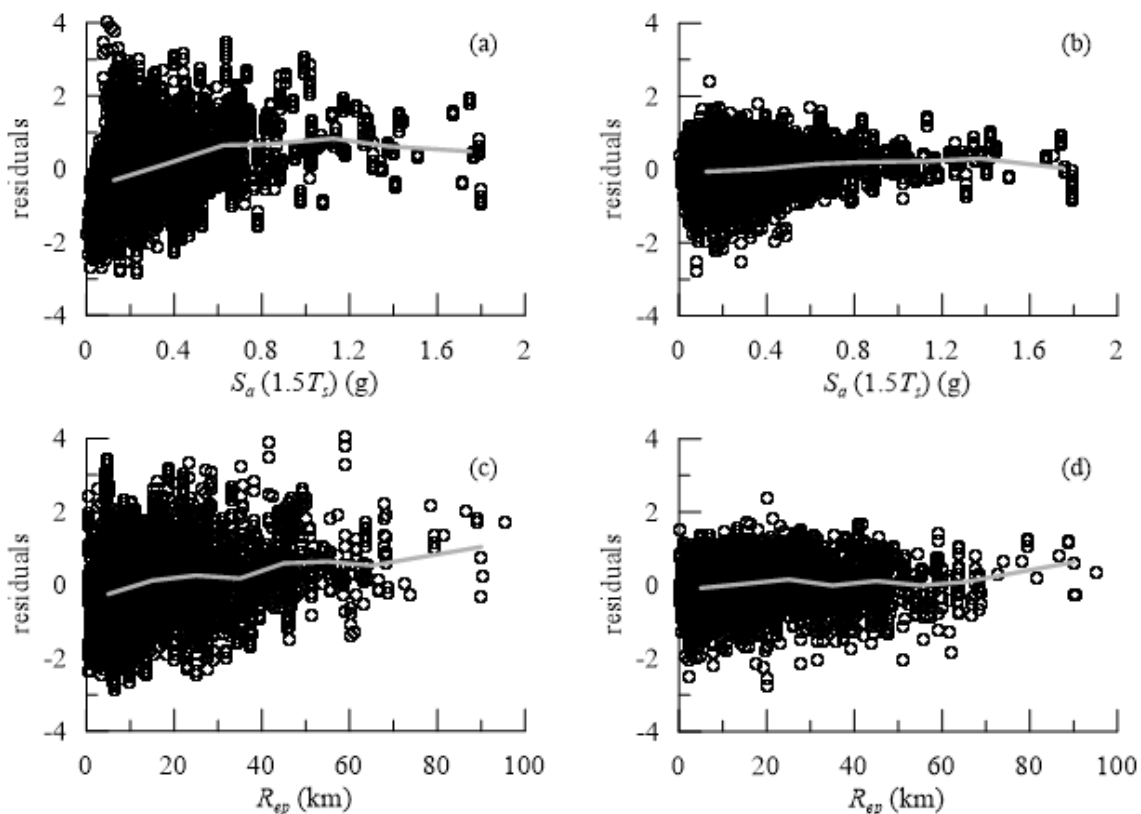
235 Figure 6. Mean residuals versus k_y/PGA for scalar approach (a) and vector approach (b) for different predictive relationships

236 As expected, Eqs. (3) and (4) provide comparable values of residuals that are significantly lower than
 237 those evaluated using the 2nd order polynomial of Saygili & Rathje (2008) of Eq. (2). The trends of
 238 Eqs. (3) and (4) are also characterised by negligible biases for increasing values of k_y/PGA , but

239 similarly to what found by Saygili & Rathje (2008), bias appears for Eq. (3) when $k_y/PGA > 0.8$,
 240 though this result is not of engineering significance due to the small displacements predicted for that
 241 level of k_y/PGA . Therefore, Figure 6 shows that the use of Eqs. (3) and (4) reduces significantly the
 242 residuals as compared with the 2nd order polynomial of Eq. (2). However, the lowest values of the
 243 mean of residuals are obtained through the new relationship proposed in this work, as shown in
 244 Figures 5 (b-d), for which no bias appear for increasing values of k_y/PGA . This is also consistent with
 245 the fact that the values of σ_{ln} reported in Table 3 obtained through Eq. (5) are lower than those
 246 computed with Eqs. (3) and (4). This is why the new proposed relationships improve the predictive
 247 capability of the permanent slope displacements as compared to the existing ones, thus being more
 248 appropriate to describe the characteristics of the Italian strong motion database. Furthermore, Figure
 249 7 and 8 show the variation of the residuals obtained from the one-parameter (PGA) and the two-
 250 parameters (PGA, PGV) models with $M_w, PGV, S_a(1.5T_s)$ and R_{ep} employing the new relationships
 251 of Eq. (5), with the greyscale lines representing the mean of residuals. As expected, the vector
 252 approach provides much lower residuals for all the considered ground motion parameters, with almost
 253 constant mean values, demonstrating that the new semi-empirical relationship proposed in this work
 254 is reasonable for the study of the Italian seismicity when using PGA and PGV as the seismic loading
 255 parameters, as it is not biased when compared to the other seismic parameters.
 256



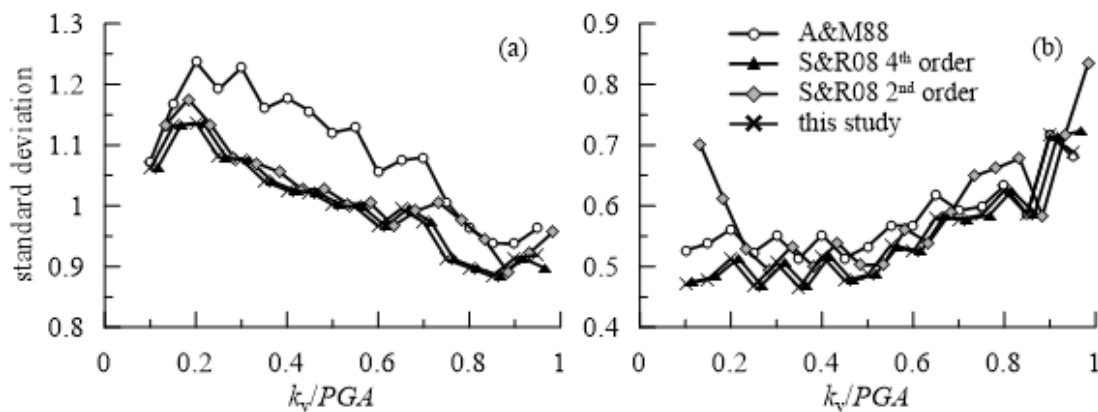
257 Figure 7. Residuals for scalar (a, c) and vector (b, d) semi-empirical relationships of Eq. (5) vs M_w and PGV



259 Figure 8. Residuals for scalar (a, c) and vector (b, d) semi-empirical relationships of Eq. (5) vs S_a and R_{ep}

260 Finally, Figure 9 gives an insight into the variation of the standard deviation with k_y/PGA for the
 261 different semi-empirical relationships: once again, σ_{ln} is significantly reduced when the PGA , PGV
 262 models are used, with the 4th order polynomial of Saygili & Rathje (2008) and the new proposal
 263 providing very similar trends and the lowest values.

264



265
 266 Figure 9. Variation of standard deviation (σ_{ln}) of displacements with k_y/PGA for (a) scalar and (b) vector relationships

267 The results presented in this section are summarised as follows. The semi-empirical relationships of
 268 Eqs. (1) and (2) are too simplistic to reproduce satisfactorily the results of the Newmark's integration

269 over a wide range of displacements and their coefficients depend on the specific values of the yield
 270 seismic coefficient. Conversely, Eqs. (3) - (5) reproduce well the calculated displacements for
 271 different values of k_y . The vector relationships provide a better description of the seismicity of the
 272 site than the scalar ones as characterised by lower values of the standard deviation. Among the
 273 presented semi-empirical relationships, the new formulation proposed in this paper should be
 274 preferred as characterised by the lowest standard deviations, by no bias in terms of residuals, while
 275 reproducing correctly the permanent displacements for k_y/PGA equal to 0 and 1.

276 **4 Probabilistic approach: effect of the predictive displacement relationships**

277 The displacement predictive equations are a key ingredient to develop the probabilistic approach,
 278 whose results are synthesised in terms of displacements hazard curves and maps, providing the annual
 279 rate of exceedance λ_d for a given level of displacement d . Here, a brief description of the probabilistic
 280 approach is presented and the reader is referred to the Appendix for further details. For the scalar
 281 approach, λ_d is calculated as:

$$\lambda_d(x) = \sum_i P[d > x | PGA_i] \times P[PGA_i] \quad (6)$$

282 with the probability of a certain displacement x $P[d > x | PGA_i]$ for a specific peak ground
 283 acceleration PGA_i , and $P[PGA_i]$ the annual probability of PGA_i provided by a probabilistic seismic
 284 hazard analysis (PSHA). In this study, the conventional scheme of PSHA proposed by [Stucchi *et al.* \(2011\)](#)
 285 for Italy is followed, in which the seismicity is uniformly distributed in each seismic source
 286 zone and the earthquake recurrence model follows the Poisson's distribution. A logic tree scheme is
 287 adopted in this scheme for the ground motion prediction equations (GMPE) and magnitude
 288 distribution. The readers are referred to the original work for further detail. Specifically, [Stucchi *et al.* \(2011\)](#)
 289 determined the values of PGA for more than 16000 points of a regular grid of 5 km
 290 throughout the Italian territory for nine probabilities of exceedance in 50 years (2%, 5%, 10%, 22%,
 291 30%, 39%, 50%, 63%, and 81%) for the 16th, 50th and 84th percentiles. The results are presented in
 292 terms of PGA hazard curves, plotting the annual rate of exceedance of this parameter against PGA ,
 293 as well as in terms of disaggregation of the PGA values for all the nine probabilities of exceedance in
 294 terms of magnitude and epicentral distance. The results are available through the webGIS interactive
 295 seismic hazard maps provided by the Italian Institute of Geophysics and Volcanology (INGV)

296 (<http://esse1.mi.ingv.it/d2.html>) that allow to extract information on the Italian territory on a regular
297 grid spaced by 0.05°.

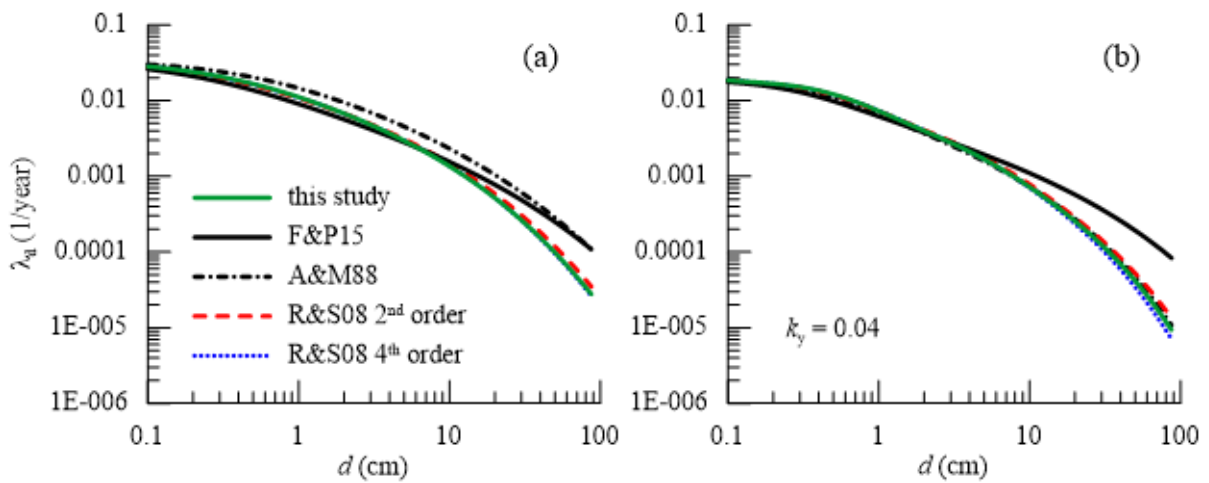
298 For the vector approach one has:

$$\lambda_d(x) = \sum_i \sum_j P[d > x | PGA_i, PGV_j] \times P[PGA_i, PGV_j] \quad (7)$$

299 where $P[d > x | PGA_i, PGV_j]$ is the probability displacements greater than x , given the peak ground
300 acceleration PGA_i and the peak ground velocity PGV_j , while $P[PGA_i, PGV_j]$ is the joint annual
301 probability of PGA_i and PGV_j . This latter term requires the disaggregation of the hazard of PGA
302 and the correlation coefficient ρ between PGA and PGV . As discussed in detail in the Appendix and
303 in [Rollo & Rampello \(2021\)](#), the correlation coefficient is evaluated through the ground motion
304 prediction equation (GMPE) of [Lanzano *et al.* \(2019\)](#), specifically developed for the Italian
305 seismicity, leading to $\rho=0.843$. Further details for the computation of [Eq. \(7\)](#) are reported in the
306 Appendix. The probabilistic approach has been implemented in the commercial numerical software
307 package MATLAB.

308 The displacement hazard curves plot the annual rate of exceedance λ_d against the displacement
309 and are presented first for the site of Amatrice (RI) in the central Italy using different yield seismic
310 coefficients and different semi-empirical relationships: [Fotopoulou & Pitalakis \(2015\)](#) (F&P15),
311 [Saygili & Rathje \(2008\)](#) (S&R08 2nd and 4th order), [Ambraseys & Menu \(1988\)](#) (A&M88) and the
312 new expression proposed herein. This permits to investigate the role of the adopted semi-empirical
313 relationships in the probabilistic framework. [Figures 10, 11 and 12](#) show the hazard curves for the
314 Italian site of Amatrice for values of $k_y=0.04, 0.08, 0.12$, respectively, for both the scalar (a) and
315 vector (b) probabilistic models. For displacements smaller than 1 to 5 cm the hazard curves obtained
316 with different predictive relationships are very similar, while for greater values some differences
317 arise.

318

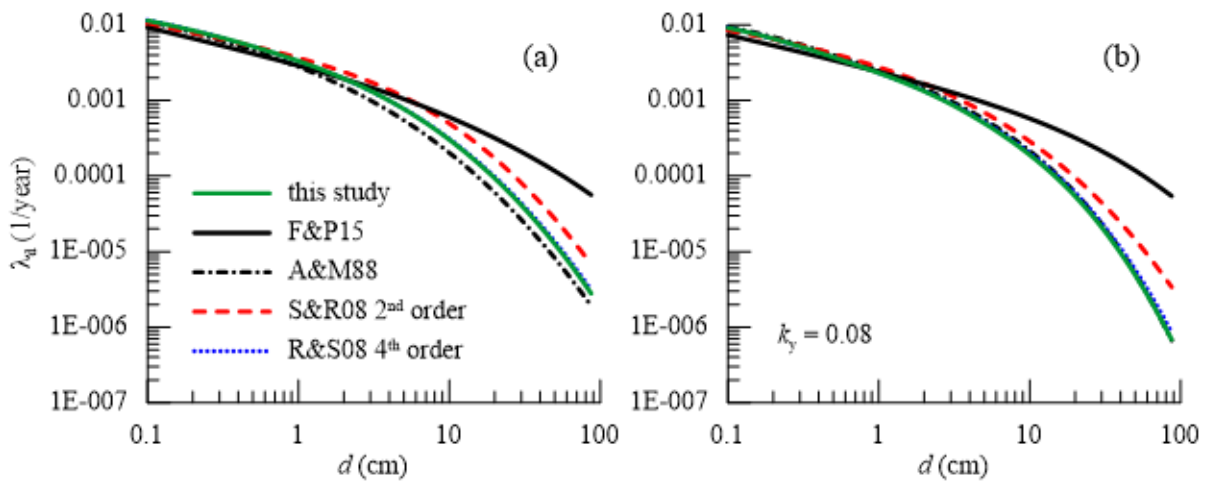


319

Figure 10. Displacement hazard curves for the site of Amatrice and $k_y = 0.04$ for (a) scalar and (b) vector models

320

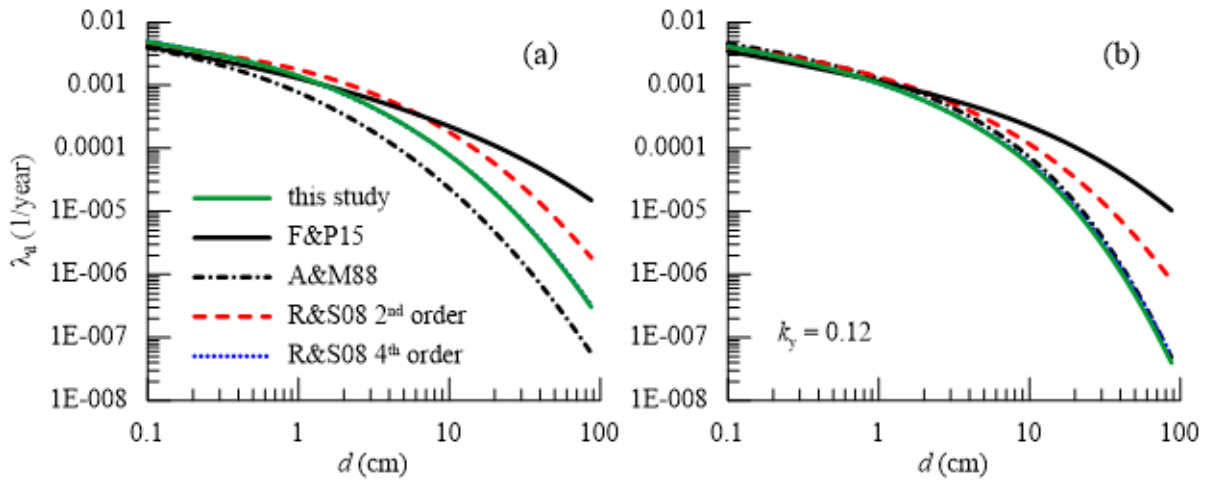
321



322

Figure 11. Displacement hazard curves for the site of Amatrice and $k_y = 0.08$ for (a) scalar and (b) vector models

323

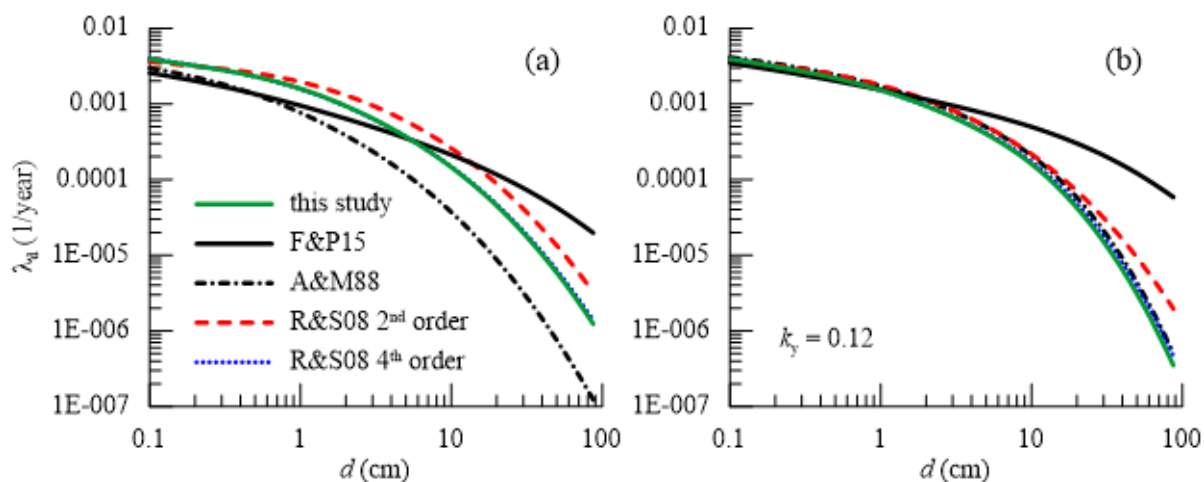


324

Figure 12. Displacement hazard curves for the site of Amatrice and $k_y = 0.12$ for (a) scalar and (b) vector models

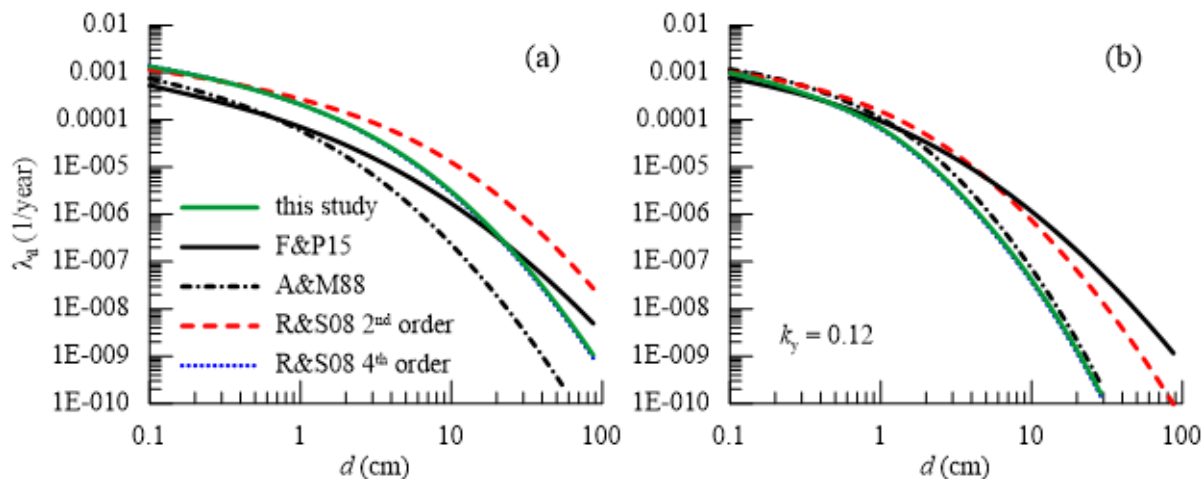
325 For the Italian site considered here, the F&P15 and the R&S08 2nd order relationships lead to the
326 largest differences in the hazard curves as compared to Eqs. (3) - (5). These results become more
327 evident as the yield seismic coefficient increases. Among the vector models, those based on the linear
328 and quadratic relationships overestimate the seismic hazard, in that lead to higher values of λ_d , and
329 are substantially affected by k_y , if compared with the two-parameters models based on Eqs. (3) - (5).
330 Eqs. (1) - (2) are simpler and provide more conservative, though less reliable results in terms of
331 hazard curves, as characterised by the highest standard deviations. On the contrary, the 4th order
332 polynomial semi-empirical relationships proposed by Saygili & Rathje (2008), that by Ambraseys &
333 Menu (1988) and the new proposed expression provide a more satisfactory estimate of the slope
334 displacements computed through the Newmark's approach, being characterised by the lowest
335 residuals. Moreover, it is seen that the displacement hazard curves obtained using the two-parameters
336 relationships of Eqs. (3) - (5) are nearly coincident, demonstrating that they predict similar results
337 when embodied in the vector probabilistic approach. By contrast, even for the two-parameters (*PGA*,
338 *PGV*) probabilistic models, the F&P15 and the R&S08 2nd order relationships are too simplistic and
339 are characterised by higher residuals. Furthermore, for the site of Amatrice Figures 10, 11 and 12
340 show that the vector approach is less sensitive to the adopted semi-empirical relationship (with the
341 exception of Eq. (1)) and hence its adoption should be preferred when developing hazard curves and
342 maps. To support and generalise the results presented till now, the analyses have been extended to
343 two other sites in Italy characterised by different seismic hazard: the site of Lioni (AV) in the southern
344 Italy and the one of Modena in the northern Italy. The displacement hazard curves obtained for $k_y =$
345 0.12 using all the semi-empirical relationships are plotted in Figures 13 and 14 for these sites,
346 permitting to draw similar conclusions to those highlighted for the site of Amatrice. The only
347 difference lies in the values of λ_d computed for a given displacement: in Figure 13 they are greater
348 than those reported in Figure 12, while those in Figure 14 are lower. This is consistent with the fact
349 that the sites of Lioni and Modena are characterised by a more and a less severe seismic hazard than
350 the site of Amatrice, respectively.

351



352 Figure 13. Displacement hazard curves for the site of Lioni and $k_y = 0.12$ for (a) scalar and (b) vector models

353



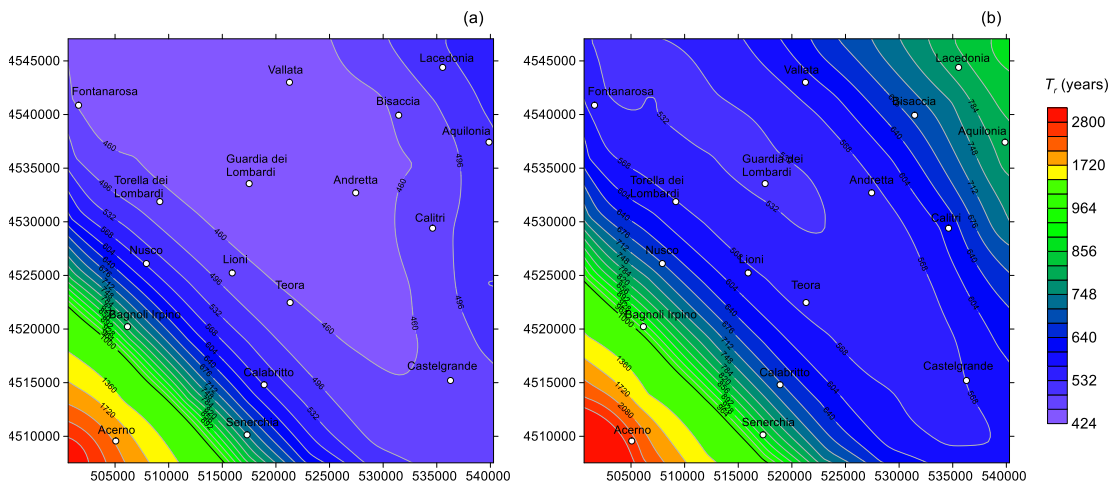
354 Figure 14. Displacement hazard curves for the site of Modena and $k_y = 0.12$ for (a) scalar and (b) vector models

355 The effect of the adopted semi-empirical relationships in the probabilistic approach is also
 356 investigated in terms of hazard maps showing the contours of the return periods T_r associated to
 357 different levels of seismic-induced displacement and yield seismic coefficients. The maps are
 358 obtained considering a grid of points equally spaced of 5 km. These points correspond to the sites on
 359 the national territory for which information pertaining to the seismic hazard in terms of *PGA* hazard
 360 curves and disaggregation are available. For any points of the map, the probabilistic analysis provides
 361 the displacement hazard curves for different values of k_y . Therefore, for a given value of k_y and a
 362 prescribed displacement, one get the corresponding value of λ_d (or $T_r = 1/\lambda_d$). The T_r values of the
 363 nearby grid points are linearly interpolated to obtain a representation in terms of return period isolines.
 364 Finally, to make the representation of results clearer, a logarithmic scale is adopted for T_r . It is worth
 365 mentioning that the maps do not account for the real distribution of the slope parameters and soils
 366 properties. However, if obtained for several values of the seismic coefficient k_y , they still represent a

367 useful tool for a preliminary assessment of the slope seismic hazard. The hazard maps presented here
 368 are developed from the vector probabilistic approach for the district of Irpinia (Campania), an area of
 369 about 40x40 km² located in the South Italy, at 50 km from the city of Naples. It is crossed by the
 370 mountain range of Apennines and is characterised by a severe seismic hazard (Porfido *et al.*, 2002;
 371 Del Gaudio & Wasowski, 2004). The x and y axes of the map are East and North according to the
 372 reference coordinate system WGS84 and the INGV interactive seismic hazard maps
 373 (<http://esse1.mi.ingv.it/d2.html>) have been used to query seismic hazard information for the points of
 374 the area of interest in terms of *PGA* hazard maps and seismic disaggregation necessary for the
 375 evaluation of Eq. (7).

376 Figures 15 and 16 refer to $k_y = 0.08$ and to threshold displacements $d_y = 2\text{cm}$ (rock-like subsoil)
 377 and $d_y = 15\text{cm}$ (free-field ductile soil behaviour) (Idriss, 1985; Wilson & Keefer, 1985), respectively.
 378 Figure 15(a) shows the results obtained through the linear relationship of Eq. (1), while Figure 15(b)
 379 shows the results computed using the new proposed relationship. The distribution of T_r is directly
 380 related to the probabilistic seismic hazard and disaggregation information of the Irpinia district, that
 381 is more severe in correspondence of the mountainous zone of the Apennines extended from North-
 382 Western to South-Eastern corners of the map.

383



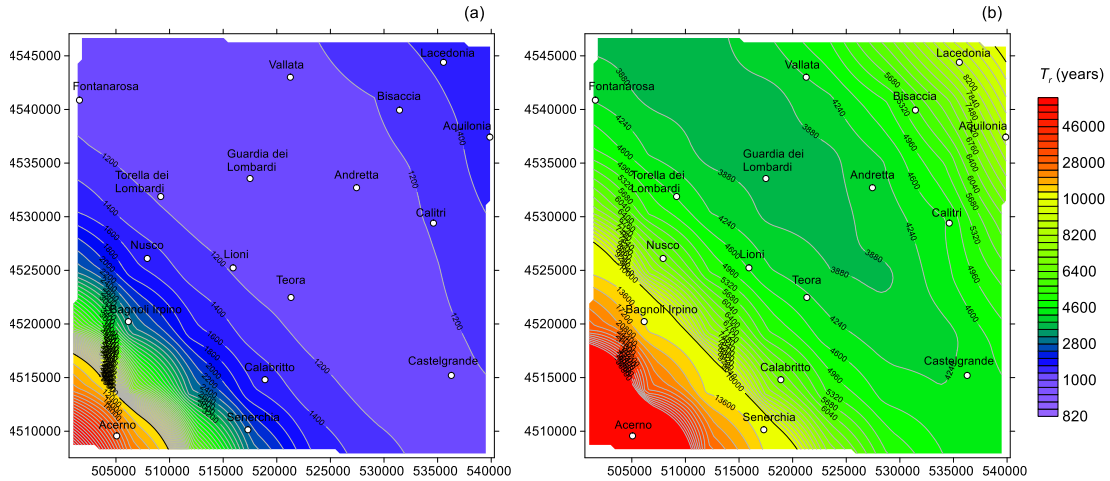
384

385 Figure 15. Displacement hazard maps for the Irpinia district for $d_y = 2\text{cm}$ and $k_y = 0.08$ for the (a) F&P15 and (b) the new proposed
 386 relationships

387 The new proposed relationship improves the prediction of the earthquake-induced displacements
 388 and, consistently with what observed in terms of hazard curves, leads to a lower hazard, that
 389 corresponds to higher values of the return period, as compared to the linear relationship. Specifically,
 390 Figure 15 shows that for roughly 40% of the map the return period increases from 430 years to 620
 391 years when the new expression is included within the probabilistic framework. Moreover, the

392 differences obtained using the two relationships become even more relevant when considering a
 393 higher threshold slope displacement $d_y = 15$ cm, as shown in Figure 16(a)-(b). Therefore, the linear
 394 relationships providing much lower return periods T_r may result in an excessively conservative
 395 estimate of the seismic hazard.

396



397

398 Figure 16. Displacement hazard maps for the Irpinia district for $d_y = 15$ cm and $k_y = 0.08$ for the (a) F&P15 and (b) the new proposed
 399 relationships

400 5 Summary and conclusions

401 This paper presents a new semi-empirical relationship that may be used to evaluate the earthquake-
 402 induced slope displacements as a function of one or two ground motion parameters and was
 403 formulated with reference to the Italian seismicity assimilating the slope to a rigid block. Five semi-
 404 empirical relationships have been compared, linking the log of displacement d and the log of the
 405 ground motion parameters PGA and PGV : (i) the linear expression by Fotopoulou & Ptilakis (2015),
 406 (ii) the second order and (iii) fourth order polynomial by Saygili & Rathje (2008), (iv) that proposed
 407 by Ambraseys & Menu (1988) and (v) the new one. The latter not only satisfies the conditions for the
 408 permanent displacements at the extrema $k_y/PGA = 0$ and $k_y/PGA = 1$ but also proves to be more
 409 efficient than other existing formulations to predict the permanent displacements as characterised by
 410 lower residuals and standard deviations when comparing the displacements calculated through the
 411 Newmark's method and the values predicted by different semi-empirical relationships. The analysis
 412 of the mean of residuals also demonstrates that differently from the existing ones, for the new
 413 relationship no bias appear for increasing values of k_y/PGA and that the residuals are almost constant
 414 within the range of values of ground motion parameters of the Italian seismic database. Moreover,
 415 the relationships analysed in this work permit to develop a scalar probabilistic approach, characterised
 416 by the single ground motion parameter PGA , or a vector approach, using the couple of parameters

417 *PGA, PGV*. The result of the analysis consists in a series of hazard curves and maps providing the
418 annual rate of exceedance associated to given values of threshold, or limit, slope displacements and
419 given values of the yield seismic coefficient k_y . The results presented in this work show that, for both
420 scalar and vector approaches, the hazard curves obtained using Eqs. (3) and (5) are similar but they
421 suggest the adoption of Eq. (5) in light of the more accurate description of the permanent
422 displacements over all the range of k_y/PGA . Moreover, the vector probabilistic approach is less
423 sensitive to the adopted displacement semi-empirical relationship and thus, in combination with Eq.
424 (5) provides a reliable assessment of the seismic hazard associated to a slope on the Italian territory.
425 It is worth recalling that the results presented in section 4 refer to specific sites and areas of Italy.
426 However, the probabilistic framework is general enough to be straightforwardly employed for any
427 other locations in Italy once information on the seismic hazard of the site are given. In principle, this
428 approach can be also extended to any geographical locations once the coefficients of the semi-
429 empirical relationships are determined based on the seismicity of the country and a proper GMPE is
430 selected. For future developments, a logic tree scheme should be introduced within the probabilistic
431 approach to account for the epistemic uncertainty coming from the slope conditions. Moreover, the
432 hazard maps could be integrated with GIS techniques to account for the spatial variability of regional
433 landslide properties. However, the results presented this study in terms of displacements hazard
434 curves and maps provide practical engineers with a powerful tool for a more rational, though
435 preliminary estimate of the seismic hazard associated to slopes.

436 **Appendix**

437 According to Rathje *et al.* (2014), for the single ground motion *PGA* displacement model the
 438 annual rate of exceedance λ_d can be computed as:

$$\lambda_d(x) = \sum_i P[d > x | PGA_i] \times P[PGA_i] \quad (A1)$$

439 To evaluate the annual rate of exceedance, the product of the two terms of Eq. (A1) has to be
 440 integrated over all the levels of *PGA* depending on the specific site under study. The first term can be
 441 computed adopting a cumulative lognormal distribution function for the permanent displacements,
 442 where the mean value is evaluated for a given value of k_y and different PGA_i according to one of the
 443 semi-empirical relationships reported in Section 2 and σ_{ln} is the standard deviation associated to the
 444 adopted equation and collected in Tables 1-3. The term $P[PGA_i]$ is obtained by differentiation of the
 445 *PGA* hazard curve available as a result of a probabilistic seismic hazard analysis (PSHA).
 446 Specifically, according to Rathje *et al.* (2014) is:

$$P[PGA_i] = \frac{\lambda(PGA_{i-1}) - \lambda(PGA_{i+1})}{2} \quad (A2)$$

447 with λ the mean rate of occurrence associated with adjacent (previous and subsequent) values of
 448 *PGA* in the *PGA* hazard curve. Therefore, there is an analogy between the probabilistic approach
 449 predicting the annual rate of exceedance λ_d of many levels of permanent displacements and a PSHA
 450 providing the annual rate of exceedance λ for different *PGA*. Given a value of displacement, the
 451 annual rate of exceedance is computed as a summation over the whole range of PGA_i that characterise
 452 the seismic hazard curve. All the values of λ_d associated to the permanent displacements d are finally
 453 plotted to obtain the displacement hazard curve.

454 For the double parameters (*PGA*, *PGV*), Rathje *et al.* (2014) suggested the following expression
 455 to determine λ_d :

$$\lambda_d(x) = \sum_i \sum_j P[d > x | PGA_i, PGV_j] \times P[PGA_i, PGV_j] \quad (A3)$$

456 where, again, the first term is the probability that $d > x$ given ground motion levels PGA_i and PGV_j
 457 determined through a cumulative lognormal distribution function for the displacement x , with the
 458 mean value and the standard deviation σ_{\ln} depending on the specific adopted displacement semi-
 459 empirical relationships and computed for the couple of parameters PGA_i and PGV_j , while the second
 460 one is the joint annual probability of occurrence of PGA_i and PGV_j . In principle, the latter should
 461 be calculated via a vector probabilistic seismic hazard analysis VPSHA (Bazzurro & Cornell, 2002),
 462 but here a simplified procedure is adopted taking advantage of the results of a standard PSHA.
 463 However, Rathje & Saygili (2009) demonstrated that the simplified approach to compute the joint
 464 probability leads to the same displacement hazard curves obtained adopting the VPSHA.

$$\begin{aligned}
 P[PGA_i, PGV_j] &= P[PGV_j | PGA_i] \times P[PGA_i] = \\
 &= \sum_k \sum_l P[PGV_j | PGA_i, M_k, R_l] \times P[M_k, R_l | PGA_i] \times P[PGA_i]
 \end{aligned}
 \tag{A4}$$

465 The conditionate probability $P[M_k, R_l | PGA_i]$ is evaluated from the disaggregation of the hazard of
 466 the specific site: for each value of PGA associated to different probabilities of exceedance, the
 467 disaggregation provides the probability for any combinations of magnitude and epicentral distance
 468 (i.e. the input is a number of i -matrices with k -rows and l -columns) to account for multiple seismic
 469 sources. The calculation of the term $P[PGV_j | PGA_i, M_k, R_l]$ requires the ground motion prediction
 470 equations (GMPE) and the correlation coefficient of PGA and PGV and is computed assuming a
 471 lognormal distribution (Bazzurro & Cornell, 2002), with specifically the mean value $\mu_{\ln PGV|PGA, M, R}$
 472 and the standard deviation $\sigma_{\ln PGV|PGA, M, R}$ evaluated as (Rathje & Saygili, 2008):

$$\begin{aligned}
 \mu_{\ln PGV|PGA, M, R} &= \mu_{\ln PGV} + \rho \frac{\sigma_{\ln PGV}}{\sigma_{\ln PGA}} (\ln PGA - \mu_{\ln PGA}) \\
 \sigma_{\ln PGV|PGA, M, R} &= \sigma_{\ln PGV} \sqrt{1 - \rho^2}
 \end{aligned}
 \tag{A5}$$

473 The terms $\mu_{\ln PGV}$, $\sigma_{\ln PGV}$, $\mu_{\ln PGA}$ and $\sigma_{\ln PGA}$ are the mean values and the standard deviations of the
 474 adopted quantities and ρ is the correlation coefficient between PGA and PGV . For the first quantities
 475 the ground motion prediction equation of Lanzano *et al.* (2019) is adopted in this paper: the mean
 476 values $\mu_{\ln PGV}$ and $\mu_{\ln PGA}$ depend on the combination of magnitude and epicentral distance (i.e. one

477 obtains a matrix of k -rows and l -columns) while $\sigma_{\ln PGV}$ and $\sigma_{\ln PGA}$ are constant and represent the
 478 standard deviations of the two ground motion parameters provided by Lanzano *et al.* (2019) that
 479 account for the epistemic uncertainty of the GMPE. For ρ the procedure by Rathje & Saygili (2008)
 480 is followed:

$$\rho = \frac{\sum_i (\varepsilon_{PGA_i} - \bar{\varepsilon}_{PGA}) (\varepsilon_{PGV_i} - \bar{\varepsilon}_{PGV})}{\sqrt{\sum_i (\varepsilon_{PGA_i} - \bar{\varepsilon}_{PGA})^2 \sum_i (\varepsilon_{PGV_i} - \bar{\varepsilon}_{PGV})^2}} \quad (A6)$$

481 where ε_{PGA} , ε_{PGV} , $\bar{\varepsilon}_{PGA}$ and $\bar{\varepsilon}_{PGV}$ are the normalised residuals for the quantities PGA , PGV and the
 482 mean value of the observed events, respectively, such that the general expression is:

$$\varepsilon_{GM} = \frac{\ln GM_{\text{observed}} - \ln GM_{\text{predicted}}}{\sigma_{\ln GM}} \quad (A7)$$

483 with GM denoting either the ground motion parameters PGA or PGV , the term $\ln GM_{\text{predicted}}$
 484 evaluated here through the ground motion prediction equation (GMPE) of Lanzano *et al.* (2019) and
 485 $\ln GM_{\text{observed}}$ depending on specific observed ground motion parameter (i.e. the values of PGA_i and
 486 PGV_j of the strong-motion database). Eq. (A6) provides a synthetic scalar value that correlates the
 487 two ground motion parameters based on the total number of observations. Given a value x of
 488 permanent displacement, the annual rate of exceedance is computed according to Eq. (A3) as a
 489 summation over the whole range of PGA_i , PGV_j , magnitude M_k and epicentral distance R_l that
 490 characterise the seismic hazard of the site.

491 The probabilistic scalar and vector approaches have been implemented in the numerical software
 492 package MATLAB. To summarise, the ingredients of the probabilistic approach are: (i) the values of
 493 displacements and the standard deviations predicted by any of the semi-empirical relationships (i.e.
 494 in this study one among Eqs. (1) – (5)), (ii) the PGA hazard curve of the site, (iii) the ground motion
 495 prediction equations for PGA and PGV in terms of mean values and standard deviations and (iv) the
 496 seismic disaggregation of PGA . Information pertaining to the seismic hazard of the specific site (i.e.
 497 PGA hazard curve and disaggregation) are provided as external input data extracted from the website
 498 of the Italian National Institute of Geophysics and Volcanology (INGV).

499

500 **Acknowledgements**

501 The research work presented in this paper was partly funded by the Italian Department of Civil
502 Protection under the ReLUIIS research project – Working Package 16: *Geotechnical Engineering* –
503 Task Group 2: *Slope stability*

504 **Conflict of interest**

505 Conflict of interest: authors declare that they have no conflict of interest.

506

507

508

509 **Notation**

510	GM	Ground motion parameter
511	a_0, a_1, \dots, a_6	Coefficients of Eqs. (1) - (4)
512	d	Permanent sliding displacement
513	d_y	Threshold permanent sliding displacement
514	I_A	Arias intensity
515	k_y	Yield seismic coefficient
516	M_w	Moment magnitude
517	PGA	Peak ground acceleration
518	PGV	Peak ground velocity
519	R_{ep}	Epicentral distance
520	$S_a(1.5T_s)$	Spectral acceleration computed at the degraded period $1.5T_s$
521	T_m	Mean period
522	T_r	Return period
523	ε_{GM}	Residual of the ground motion parameter
524	λ_d	Displacement annual rate of exceedance
525	μ_{ln}	Natural log of mean value
526	ρ	Correlation coefficient
527	σ_{ln}	Natural log of standard deviation

528 **References**

- 529 Ambraseys, N. N., & Menu, J. M. (1988). Earthquake- induced ground displacements. *Earthquake engineering &*
530 *structural dynamics*, 16(7), 985-1006.
- 531 Bazzurro, P., and Cornell, C. A. (2002). Vector-valued probabilistic seismic hazard analysis (VPSHA). *Proc., 7th U.S.*
532 *National Conf. on Earthquake Engineering*, Vol. II, EERI, Oakland, Calif., 1313–1322.
- 533 Biondi, G., Cascone, E., Rampello, S. (2011). Valutazione del comportamento dei pendii in condizioni sismiche. *Rivista*
534 *italiana di geotecnica*, 45(1), 9-32.
- 535 Bradley, B. A. (2012). The seismic demand hazard and importance of the conditioning intensity measure. *Earthquake*
536 *Engineering & Structural Dynamics*, 41(11), 1417-1437.
- 537 Bray, J. D., Macedo, J., & Travarasrou, T. (2018). Simplified procedure for estimating seismic slope displacements for
538 subduction zone earthquakes. *Journal of Geotechnical and Geoenvironmental Engineering*, 144(3), 04017124.
- 539 Bray, J. D., & Macedo, J. (2019). Procedure for estimating shear-induced seismic slope displacement for Shallow Crustal
540 Earthquakes. *Journal of Geotechnical and Geoenvironmental engineering*, 145(12), 04019106.
- 541 CEN (Comité Européen de Normalisation) (2003) prEN 1998-1- Eurocode 8: design of structures for earthquake
542 resistance. Part 1: General rules, seismic actions and rules for buildings. Draft No 6, Doc CEN/TC250/SC8/N335,
543 January 2003, Brussels.
- 544 Cho, Y., & Rathje, E. M. (2022). Generic Predictive Model of Earthquake-Induced Slope Displacements Derived from
545 Finite-Element Analysis. *Journal of Geotechnical and Geoenvironmental Engineering*, 148(4), 04022010.
- 546 Chousianitis, K., Del Gaudio, V., Kalogeras, I., Ganas, A. (2014). Predictive model of Arias intensity and Newmark
547 displacement for regional scale evaluation of earthquake-induced landslide hazard in Greece. *Soil Dynamics and*
548 *Earthquake Engineering*, 65, 11-29.
- 549 Chousianitis, K., Del Gaudio, V., Sabatakakis, N., Kavoura, K., Drakatos, G., Bathrellos, G. D., Skilodimou, H. D. (2016).
550 Assessment of Earthquake- Induced Landslide Hazard in Greece: From Arias Intensity to Spatial Distribution of
551 Slope Resistance Demand Assessment of Earthquake- Induced Landslide Hazard in Greece. *Bulletin of the*
552 *Seismological Society of America*, 106(1), 174-188.
- 553 Cornell C. A., Luco, N. (2001). Ground motion intensity measures for structural performance assessment at near-fault
554 sites: In *Proceedings of the U.S.-Japan joint workshop and third grantees meeting, U.S.-Japan cooperative research*
555 *on urban earthquake disaster mitigation*. Seattle: Washington.
- 556 Del Gaudio, V., Wasowski, J. (2004). Time probabilistic evaluation of seismically induced landslide hazard in Irpinia
557 (Southern Italy). *Soil Dynamics and Earthquake Engineering*, 24(12), 915-928.
- 558 Du, W., Wang, G. (2016). A one-step Newmark displacement model for probabilistic seismic slope displacement hazard
559 analysis. *Engineering Geology*, 205, 12-23.
- 560 Du, W., Wang, G., & Huang, D. (2018a). Evaluation of seismic slope displacements based on fully coupled sliding mass
561 analysis and NGA-West2 database. *Journal of Geotechnical and Geoenvironmental Engineering*, 144(8), 06018006.
- 562 Du, W., Wang, G., & Huang, D. (2018b). Influence of slope property variabilities on seismic sliding displacement
563 analysis. *Engineering geology*, 242, 121-129.
- 564 Gaudio, D., Rauseo, R., Masini L., Rampello, S. (2020). Semi-empirical relationships to assess the seismic performance
565 of slopes from an updated version of the Italian seismic database. *Bulletin of Earthquake Engineering*, published on
566 line 28/08/2020, doi.org/10.1007/s10518-020-00937-6.
- 567 Fotopoulou, S. D., & Pitilakis, K. D. (2015). Predictive relationships for seismically induced slope displacements using
568 numerical analysis results. *Bulletin of Earthquake Engineering*, 13(11), 3207-3238.
- 569 Idriss, I.M. (1985). Evaluating seismic risk in engineering practice. In: *Proceedings of the eleventh international*
570 *conference on soil mechanics and foundation engineering*, San Francisco, CA, pp 255–320.

- 571 Jibson, R. W. (2007). Regression models for estimating coseismic landslide displacement. *Engineering geology*, 91(2-4),
572 209-218.
- 573 Jibson, R. W. (2011). Methods for assessing the stability of slopes during earthquakes—A retrospective. *Engineering*
574 *Geology*, 122(1-2), 43-50.
- 575 Kan, M. E., Taiebat, H. A., & Taiebat, M. (2017). Framework to assess Newmark-type simplified methods for evaluation
576 of earthquake-induced deformation of embankments. *Canadian Geotechnical Journal*, 54(3), 392-404.
- 577 Lanzano, G., Luzi, L., Pacor, F., Felicetta, C., Puglia, R., Sgobba, S., D'Amico, M. (2019). A Revised Ground- Motion
578 Prediction Model for Shallow Crustal Earthquakes in Italy. *Bulletin of the Seismological Society of America*, 109(2),
579 525-540.
- 580 Lari, S., Frattini, P., Crosta, G. B. (2014). A probabilistic approach for landslide hazard analysis. *Engineering*
581 *geology*, 182, 3-14.
- 582 Li, D. Q., Wang, M. X., & Du, W. (2020). Influence of spatial variability of soil strength parameters on probabilistic
583 seismic slope displacement hazard analysis. *Engineering Geology*, 276, 105744.
- 584 Li, C., Wang, G., He, J., & Wang, Y. (2022). A novel approach to probabilistic seismic landslide hazard mapping using
585 Monte Carlo simulations. *Engineering Geology*, 301, 106616.
- 586 Liu, C., & Macedo, J. (2022). Machine learning-based models for estimating seismically-induced slope displacements in
587 subduction earthquake zones. *Soil Dynamics and Earthquake Engineering*, 160, 107323.
- 588 Macedo, J., & Candia, G. (2020). Performance-based assessment of the seismic pseudo-static coefficient used in slope
589 stability analysis. *Soil Dynamics and Earthquake Engineering*, 133, 106109.
- 590 Macedo, J., Candia, G., Lacour, M., & Liu, C. (2020). New developments for the performance-based assessment of
591 seismically-induced slope displacements. *Engineering Geology*, 277, 105786.
- 592 Meehan, C. L., & Vahedifard, F. (2013). Evaluation of simplified methods for predicting earthquake-induced slope
593 displacements in earth dams and embankments. *Engineering Geology*, 152(1), 180-193.
- 594 Newmark, N. M. (1965). Effects of earthquakes on dams and embankments. *Geotechnique*, 15(2), 139-160.
- 595 Porfido, S., Esposito, E., Vittori, E., Tranfaglia, G., Michetti, A. M., Blumetti, M., Serva, L. (2002). Areal distribution of
596 ground effects induced by strong earthquakes in the Southern Apennines (Italy). *Surveys in Geophysics*, 23(6), 529-
597 562.
- 598 Rampello, S., Callisto, L., Fargnoli, P. (2010). Evaluation of slope performance under earthquake loading
599 conditions. *Rivista Italiana di Geotecnica*, 44(4), 29-41.
- 600 Rathje, E. M., Saygili, G. (2008). Probabilistic seismic hazard analysis for the sliding displacement of slopes: scalar and
601 vector approaches. *Journal of Geotechnical and Geoenvironmental Engineering*, 134(6), 804-814.
- 602 Rathje, E. M., & Saygili, G. (2009). Probabilistic assessment of earthquake-induced sliding displacements of natural
603 slopes. *Bulletin of the New Zealand Society for Earthquake Engineering*, 42(1), 18-27.
- 604 Rathje, E. M., & Saygili, G. (2011). Estimating fully probabilistic seismic sliding displacements of slopes from a
605 pseudoprobabilistic approach. *Journal of Geotechnical and Geoenvironmental Engineering*, 137(3), 208-217.
- 606 Rathje, E. M., Wang, Y., Stafford, P. J., Antonakos, G., Saygili, G. (2014). Probabilistic assessment of the seismic
607 performance of earth slopes. *Bulletin of Earthquake Engineering*, 12(3), 1071-1090.
- 608 Rodriguez-Marek, A., Song, J. (2016). Displacement-based probabilistic seismic demand analyses of earth slopes in the
609 near-fault region. *Earthquake Spectra*, 32(2), 1141-1163.
- 610 Rollo, F., Rampello, S. (2021). Probabilistic assessment of seismic-induced slope displacements: an application in
611 Italy. *Bull Earthquake Eng.* <https://doi.org/10.1007/s10518-021-01138-5>.
- 612 Saygili, G., Rathje, E. M. (2008). Empirical predictive models for earthquake-induced sliding displacements of
613 slopes. *Journal of geotechnical and geoenvironmental engineering*, 134(6), 790-803.

614 Saygili, G., Rathje, E. M. (2009). Probabilistically based seismic landslide hazard maps: an application in Southern
615 California. *Engineering Geology*, 109(3-4), 183-194.

616 Sharifi-Mood, M., Olsen, M. J., Gillins, D. T., Mahalingam, R. (2017). Performance-based, seismically-induced landslide
617 hazard mapping of Western Oregon. *Soil Dynamics and Earthquake Engineering*, 103, 38-54.

618 Song, J., Gao, Y., Rodriguez-Marek, A., Feng, T. (2017). Empirical predictive relationships for rigid sliding displacement
619 based on directionally-dependent ground motion parameters. *Engineering Geology*, 222, 124-139.

620 Song, J., Gao, Y., & Feng, T. (2018). Probabilistic assessment of earthquake-induced landslide hazard including the
621 effects of ground motion directionality. *Soil Dynamics and Earthquake Engineering*, 105, 83-102.

622 Stucchi, M., Meletti, C., Montaldo, V., Crowley, H., Calvi, G. M., & Boschi, E. (2011). Seismic hazard assessment (2003–
623 2009) for the Italian building code. *Bulletin of the Seismological Society of America*, 101(4), 1885-1911.

624 Tropeano, G., Silvestri, F., Ausilio, E. (2017). An uncoupled procedure for performance assessment of slopes in seismic
625 conditions. *Bulletin of Earthquake Engineering*, 15(9), 3611-3637.

626 Wang, Y., Rathje, E. M. (2015). Probabilistic seismic landslide hazard maps including epistemic uncertainty. *Engineering
627 Geology*, 196, 313-324.

628 Wang, Y., & Rathje, E. M. (2018). Application of a probabilistic assessment of the permanent seismic displacement of a
629 slope. *Journal of Geotechnical and Geoenvironmental Engineering*, 144(6), 04018034.

630 Wang, M. X., Huang, D., Wang, G., & Li, D. Q. (2020). SS-XGBoost: a machine learning framework for predicting
631 newmark sliding displacements of slopes. *J Geotech Geoenviron Eng*, 146(9), 04020074.

632 Wang, M. X., Li, D. Q., & Du, W. (2021). Probabilistic Seismic Displacement Hazard Assessment of Earth Slopes
633 Incorporating Spatially Random Soil Parameters. *Journal of Geotechnical and Geoenvironmental
634 Engineering*, 147(11), 04021119.

635 Wasowski, J., Keefer, D. K., & Lee, C. T. (2011). Toward the next generation of research on earthquake-induced
636 landslides: current issues and future challenges. *Engineering Geology*, 122(1-2), 1-8.

637 Wilson, R.C., Keefer, D.K. (1985). Predicting areal limits of earthquake-induced landsliding. In: Ziony ED (ed)
638 Evaluating Earthquake Hazard in the Los Angeles Region. US Geological Survey, Reston, pp 317–345.

639 Xiong, M., & Huang, Y. (2019). Novel perspective of seismic performance-based evaluation and design for resilient and
640 sustainable slope engineering. *Engineering Geology*, 262, 105356.

641 Yeznabad, A. F., Molnar, S., El Naggari, M. H., & Ghofrani, H. (2022). Estimation of probabilistic seismic sliding
642 displacement and pseudo-static coefficients (k15) for seismic stability assessment of slopes in the southern Lower
643 Mainland, British Columbia. *Soil Dynamics and Earthquake Engineering*, 161, 107364.